Tanzania Journal of Science 49(4): 831-841, 2023
ISSN 0856-1761, e-ISSN 2507-7961

A Computational Study on the Impact of Anchoring Groups on the Optical and Electronic Properties of Triphenylamine-Based Dyes for Dye-Sensitized Solar Cell Applications

Geradius Deogratias* and Grace Kinunda
Chemistry Department, University of Dar es Salaam, P.O. Box 35061, Dar es Salaam, Tanzania.
Corresponding author, e-mail: dgeradius@gmail.com, dgeradius@udsm.ac.tz
Received May 2023, Revised 2 Aug 2023, Accepted 23 Aug 2023 Published Oct 2023
DOI: https://dx.doi.org/10.4314/tjs.v49i4.5

Abstract

Anchoring groups are crucial for enhancing the performance of dye-sensitized solar cells (DSSCs). For instance, cyanoacrylic acid serves as the primary anchoring group in DSSC due to its crucial elements required for effective electron transport. However, it suffers from degradation. To address this limitation, this study proposes alternative cyano-based anchoring groups for sensitizers. Density functional theory (DFT) and time-dependent DFT were used to investigate the optical and electronic properties of the dyes. The studied dyes (excluding the dye containing OH group) displayed three absorption bands within the visible and NIR regions. Low-energy peaks ranged from 498 to 576 nm, corresponding to excitation from ground state to first excited state. Moderate intensity bands appeared at 376 to 418 nm, with the highest energy bands falling within 351 to 384 nm. Ground state oxidation potential values for the dyes were lower than the redox potential of the iodide/triiodide pair. Similarly, excited state oxidation potential values were higher than or equal to the conduction band of TiO_2, except for NO_2 and CHO containing dyes. Ionization potential values ranged from 6.24 eV to 6.40 eV, while electron affinity values were within 1.21 eV to 2.74 eV. Chemical potential values ranged from 3.75 to 4.57 eV, and chemical hardness of the dyes fell between 1.83 to 2.54 eV. The proposed cyano-based anchoring groups show promising potential for enhancing DSSC performance.

Keywords: Anchoring groups, Sensitizers, Optoelectronic, Solar energy, Charge transfer.

Introduction

Solar energy is a highly abundant and widely available form of renewable energy that has the potential to significantly contribute to the mitigation of the global energy crisis caused by the depletion of fossil fuels and the increasing demand for energy (Wang et al. 2020). Its abundance is evident from the fact that an estimated power of approximately 1.8×10^{11} MW hits the Earth's surface (Parida et al. 2011). Despite the vast amount of solar energy that strikes the Earth's surface, solar energy only contributed approximately 8.7% to the total global energy mix in 2019 (IEA 2020). The solar energy industry is facing challenges due to lack of appropriate light-harvesting materials, limited resources (such as silicon, land for solar panel installation, and rare earth metals used in some types of solar panels), and the high costs of fabricating solar cells (Mariotti et al. 2020, Sharma et al. 2018). The use of Dye-Sensitized Solar Cells (DSSCs) has recently gained attention as a promising technology that could potentially transform the energy industry (Ikpesu et al.

2020, Liu et al. 2020). The type of solar cells has gained widespread attention as a promising alternative to traditional silicon-based solar cells due to their advantageous features such as flexibility, lightweight, tunable aesthetic features of vivid colours, transparency, relative high photovoltaic efficiencies, non-toxicity, environmental friendliness, low cost and straightforward synthesis (Pathak et al. 2019, Deogratias et al. 2020a, Zhang et al. 2020).

The sensitizers' architectural design comprises the donor moiety (D), π-spacers/linkers and the anchoring groups (A) in the D-π-A order (Zhao et al. 2021). Other architectural motifs include D-π-A-π-A (Elmorsy et al. 2018, Luo et al. 2016), D-A-A (Wu et al. 2015), D-A-π-A (Cui et al. 2011, Tian et al. 2015, Zhang et al. 2018a, 2018b), 2D-π-2A (Jia et al. 2019) and D-π-π-A (Deogratias et al. 2020b, 2020c). These architectures have been reported to enhance the optoelectronic properties of sensitizers. A good progress has been realized in development of effective electron donor group such as indoline (Horiuchi et al. 2004), carbazole (Lokhande et al. 2019, Xu et al. 2014), coumarin (Shkoor et al. 2020), and triphenylamine (TPA) (Irfan 2019, Wan et al. 2021), the π-bridges for example pyrrole, thiophene, oligo-phenylenevinylene and furan and anchoring groups such as carboxylic acid and rhodamine (Wan et al. 2017).

The anchoring groups play an important role in the stability of DSSCs by preventing photo-degradation and in facilitating the higher charge injection efficiency through their bonding with the semiconductor surface (Zhang et al. 2018a, 2018b, Maddah et al. 2020). The impact of anchoring groups on the photochemical properties of dyes and the overall performance of DSSC has been widely studied and reported by a number of researchers (Deogratias et al. 2020a, 2020b, Slimi et al. 2020). The choice of anchoring groups is crucial in determining the stability of the DSSC against photo-degradation and in facilitating the efficient injection of charges from the sensitizer into the semiconductor surface. The cyanoacrylic acid (CA) anchoring group is commonly used in DSSCs. However, it has been found that these groups can dissociate when exposed to water or prolonged illumination, thus can negatively impacting the loading of the dye and reduce the overall power conversion efficiency (PCE) of the devices.

The limitations of cyanoacrylic acid have led scientists to search for alternative anchoring groups with better binding energy to the semiconductor surface. For instance, Zhao et al. (2021) reported on the use of acyclic anchoring groups, specifically a set of dyes SPL301-SPL307, which have shown improved binding energy and wider absorption bands compared to cyanoacrylic acid. The work of Guo and colleagues (2016) showed that using a heterocyclic anchoring group (hydantoin) instead of CA in combination with methoxy-substituted TPA could improve the PCE of DSSCs (Guo et al. 2016). The PCE for the hydantoin-containing dye was found to be ~8%, which is higher than the ~5% obtained for the CA-containing dye. In recent studies, it was theoretically found that the inclusion of chalcogenide π-linkers can improve the optical and electronic properties of DSSCs. This modification resulted in a bathochromic shift, with the order of O < S < Se < Te (Deogratias et al. 2020a, 2020b, 2022, 2023). The π-linkers which contain sulfur such as thiophene and benzothiadiazole, are commonly used to promote intramolecular charge transfer in sensitizers. This work explores the effects of cyano-based anchoring groups as alternatives to the traditional cyanoacrylic acid anchoring group for dyes featuring methoxy-substituted TPA, thiophene, and benzothiadiazole as π-linkers, as shown in Figure 1. This computational investigation offers promising dyes that could potentially improve the performance of DSSC technology, opening new avenues for more efficient and sustainable solar energy conversion.

Materials and Methods

Materials

The present study focused on the use of methoxy-substituted TPA with thiophene and benzothiadiazole as π-linkers, in combination with specific anchoring groups as depicted in Figure 1, to enhance the optical and electronic characteristics of DSSCs.

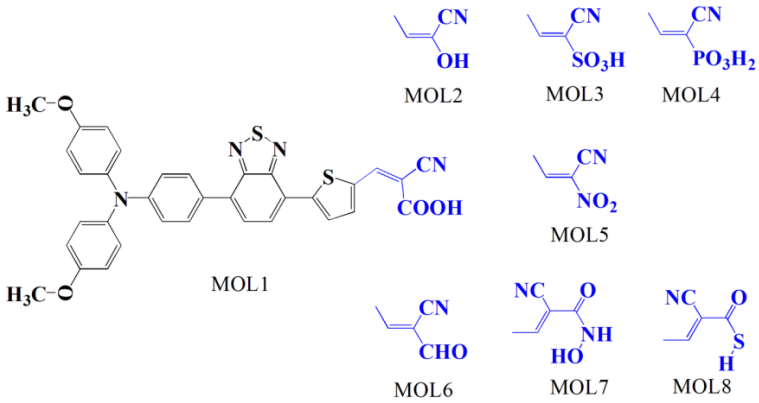

Figure 1: The explored chemical structures feature cyano-based anchoring groups with methoxy-substituted triphenylamine, thiophene, and benzothiadiazole π-linkers.

The results reported were obtained using a desktop computer powered by a 4-core, 8-thread Intel Core i7-7700 CPU with 8 MB of cache and a base frequency of 3.60 GHz. The Windows 10 64-bit was the operating system with 32 GB of DDR4 RAM running at 2400 MHz to facilitate memory-intensive activities. In order to generate the coordinates, the three-dimensional geometries were created using the Avogadro program (Hanwell et al. 2012) and then energy was reduced using the universal force field (UFF) available within the package. The minimum conformational energy coordinates were used as inputs for full optimization using Gaussian 16 (Frisch et al. 2016) to obtain the equilibrium geometries.

Methods

This computational study involved investigating optical and electronic properties of the proposed chemical structures using density functional theory (DFT) and time-dependent DFT (TD-DFT). The optimization of the structures was carried out using the B3LYP functional (Becke 1996) coupled with 6-31+G(d,p) basis set. The choice for the functional and basis set for simulation of electronic spectra were obtained by following the methodology as previously described (Deogratias et al. 2020a). The electronic spectra were simulated using a combination of CAM-B3LYP (Yanai et al. 2004) functional and basis sets, specifically 6-31+G(d,p) which have been shown to accurately reproduce experimental observations for reference molecule, MOL1. All calculations were conducted in chloroform solvent using a polarized continuum model (PCM) (Miertuš et al. 1981, Cammi and Tomasi 1995, Barone and Cossi 1998).

Results and Discussion

Absorption properties

The effectiveness of a dye in a DSSC relies on its ability to absorb light in the visible and near-infrared (NIR) regions. In this study, the absorption spectra of the investigated dyes were determined using the TD-DFT method, and the results are presented in Figure 2. Their spectral peaks (λ_{max}), excitation energies (E_x), oscillator strengths (f), light harvesting efficiencies (LHE), excited-state lifetime (τ) and molecular orbital contribution are summarized in Table 1.

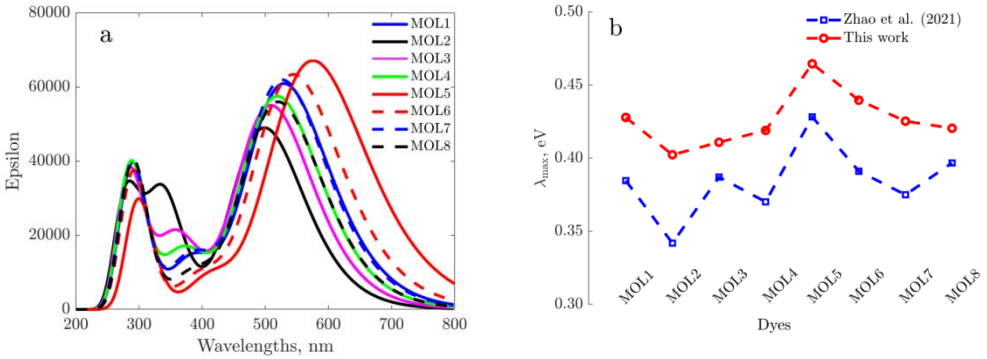

Figure 2: (a) Simulated UV-Vis absorption spectra (b) comparison of maximum absorption wavelengths with literature data (Zhao et al. 2021).

From Figure 2(a), it is apparent that the investigated dyes demonstrate three prominent absorption bands within the visible and NIR regions. The low-energy peaks, ranging from 498 to 576 nm. The λ_{max} values for all dyes primarily correspond to the transition from the ground state to the first-excited state ($s_0 \rightarrow s_1$), which is predominantly observed from the highest occupied molecular orbital (HOMO) to the lowest unoccupied molecular orbital (LUMO). This transition accounted for more than 59% of the overall contribution. The moderate energy bands were observed at 376 to 418 nm, while the highest energy bands were found in the range of 351 to 384 nm. The absorption in the low energy bands can be attributed to the localized $\pi \rightarrow \pi^*$ electron migration from the TPA-based donor moiety to the acceptor unit, as previously reported (Guo et al. 2016, Panneerselvam et al. 2017), and the high energy bands may be attributed to $n \rightarrow \pi^*$ transition. The red-shift observed in the electronic spectra showed a positive correlation with the shift in the HOMO energies, as represented by the equation $E_x = 2.035 \times E_{HOMO} + 15.224$ (with $R^2 = 0.88$), compared to the weaker correlation observed with the LUMO energies ($E_x = 0.162 \times E_{LUMO} + 2.706$, $R^2 = 0.53$). It is worth noting that among the studied dyes, MOL2, which features a hydroxyl substitution in the anchoring group, had the lowest and blue-shifted absorption peaks. On the other hand, the dye with NO_2 substitution (MOL5) is the most red-shifted with highest intensity, which is consistent with previous literature (Zhao et al. 2021). The maximum wavelengths of the studied dyes follow the order of MOL5 > MOL6 > MOL1 > MOL7 > MOL8 > MOL4 > MOL3 > MOL2. It is evident that the addition of π-linkers in the dyes with a D-π-π-A configuration has improved the λ_{max} values compared to similar dyes with a D-π-A configuration, as shown in Figure 2(b). The light-harvesting efficiency (LHE) values were all above 0.94 (Table 1) indicating excellent light absorption ability among the studied dyes. The excited-state lifetime in DSSCs represents the duration during which an electron remains in an excited state following light absorption. This parameter plays a critical role as it governs the available time for the injected electron to undergo charge separation and actively contribute to the generation of photocurrent.

The excited-state lifetime (τ) was determined using the formula: $\tau = \frac{1.499}{f \times E_x^2}$, where the units of E_x are given in cm^{-1}. The τ values of the studied dyes were determined to be in the range of 2.74 to 3.08 nanoseconds. It is worth noting that MOL5, which exhibited the most red-shifted electronic spectra, had the second-highest τ value of 3.01 ns after MOL2. A longer excited-state lifetime is highly advantageous since it reduces the likelihood of charge recombination, thereby enhancing the overall efficiency of the DSSC.

Table 1: Maximum absorption wavelengths (λ_{max}, nm), corresponding oscillator strength wavelength (*f*), light-harvesting efficiency (LHE,%), excited-state lifetime (τ, ns) and transition assignments of isolated dyes

Dye	λ_{max}	*f*	LHE	τ	Contributions
MOL1	531	1.50	0.97	2.82	H→L (60%), H−1→L (32%)
MOL2	499	1.21	0.94	3.08	H→L (61%), H−1→L (31%),
MOL3	510	1.36	0.96	2.87	H→L (60%), H−1→L (32%)
MOL4	520	1.42	0.96	2.85	H→L (60%), H−1→L (32%)
MOL5	576	1.65	0.98	3.01	H→L (59%), H−1→L (31%)
MOL6	545	1.56	0.97	2.85	H→L (59%), H-1→L (32%)
MOL7	527	1.52	0.97	2.74	H→L (60%), H→1−L (32%)
MOL8	521	1.38	0.96	2.95	H→L (59%), H→1−L (33%)

Energy level alignment

Spontaneous charge transfer processes in DSSCs require the appropriate alignment of energy levels. Therefore, precise alignment of energy levels is necessary for the occurrence of these spontaneous charge transfer processes. Despite the occurrence of charge transfer and optical transitions involving multiple electrons in excited states, as indicated in Table 1, these phenomena are frequently simplified as single electron transitions between the HOMO and LUMO levels in the majority of density functional theory calculations. Therefore, examining the energy levels of the LUMO and HOMO is crucial for predicting various properties of sensitizers as these levels are affected by the structural modifications (Arkan et al. 2015). In order to achieve efficient charge injection from the excited dye to the conduction band of the semiconductor, it is imperative for the energy of the excited-state oxidation potential (ESOP) of the dye to be more positive than the semiconductor's conduction band ($E_{CB}^{TiO_2} = -4.05$ eV) (Fujisawa et al. 2017); excited state oxidation potential (ESOP) is determined by summing ground state oxidation potential (GSOP) and E_x, with GSOP being synonymous with the HOMO. The extent of spontaneous charge injection process is ascertained by evaluating the free energy of charge injection (ΔG_{inj}), calculated as the difference between the $E_{CB}^{TiO_2}$ and the ESOP. Likewise, the dye regeneration process becomes viable when the GSOP is more negative than electrolyte's redox couple potential ($E_{I^-/I_3^-} = -4.8$ eV). The degree of dye regeneration is quantified by the free energy of dye regeneration (ΔG_{reg}), where ΔG_{reg} is calculated as the difference between GSOP and E_{I^-/I_3^-}. Figure 3 illustrates the energy alignment diagram for the investigated dyes, showcasing the distribution of energy levels. Additionally, Table 2 provides a comprehensive summary of the energetics associated with charge transfer properties.

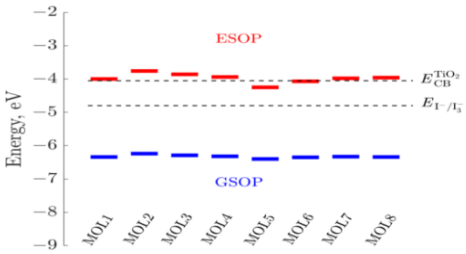

Figure 3: Schematic representation of the energy level alignment between the investigated sensitizers, the TiO_2 conduction band, and the redox potential of the iodide/triiodide pair.

The GSOP values for all the studied dyes were lower than redox potential of the iodide/triiodide pair, in similar manner, ESOP were greater or equal to conduction band of TiO_2 with exception to MOL5 and a similar trend of all other molecular orbitals were observed in comparison to literature dyes with single π−spacer (Zhao et al. 2021). These energy alignments are important to ensure there are sufficient driving forces in the DSSC to allow charge transfer processes including charge injection and dye regeneration.

Table 2: Energetics characterizing charge transfer properties, encompassing excitation energy (E_x), free energy of injection (ΔG_{inj}) and free energy of dye regeneration (ΔG_{reg}), all measured in electron volts (eV).

Dye	E_x	ΔG_{inj}	$-\Delta G_{reg}$
MOL1	2.34	−0.05	1.54
MOL2	2.48	−0.29	1.44
MOL3	2.43	−0.19	1.49
MOL4	2.38	−0.11	1.52
MOL5	2.15	+0.20	1.60
MOL6	2.28	+0.02	1.55
MOL7	2.35	−0.07	1.53
MOL8	2.38	−0.09	1.54

From a thermodynamic standpoint, negative driving forces are necessary for the initiation of a spontaneous charge transfer process. The computed ΔG_{inj} values ranged from −0.29 to 0.20 eV. From the data reported in Table 2, it is evident that the majority of the dyes exhibit negative values for ΔG_{inj}, indicating favourable conditions for spontaneous charge transfer processes with exception to MOL5 and MOL6. The studied dyes exhibit E_x values ranging from 2.34 eV to 2.48 eV, with the corresponding ΔG_{inj} values ranging from −0.29 eV to −0.05 eV. In contrast, MOL5 and MOL6 deviate from this trend, displaying positive ΔG_{inj} values (0.2 eV for MOL5 and 0.02 eV for MOL6). This discrepancy suggests less favourable charge transfer properties, emphasizing the need for further investigation to optimize their performance. In contrast to ΔG_{inj} which shows notable variation, the values of ΔG_{reg} exhibit a more moderate range with standard deviations of 0.04 and 0.13 for ΔG_{reg} and ΔG_{inj}, respectively. The relatively low standard deviation suggests that the regeneration process is less affected by changes in the investigated anchoring group, indicating that the efficiency of dye regeneration remains relatively stable across the studied dyes.

Global chemical reactivity descriptors

The ionization potential (IP) and electron affinity (EA) were employed as the basis for deriving global chemical reactivity descriptors, in accordance with Koopman's theorem (Sun et al. 2015, Gayathri 2018). The IP, EA, and additional global chemical reactivity descriptors, including the electrophilicity index (ω), electrodonating power (ω^-), electroaccepting power (ω^+), chemical potential (μ), and chemical hardness (η) were assessed in the following manner: $EA = -LUMO$, $IP = -HOMO$, $\mu = -\frac{1}{2}(IP + EA)$, $\eta = \frac{1}{2}(IP - EA)$, $\omega = \frac{\mu^2}{2\eta}$, $\omega^- \approx \frac{(3IP + EA)^2}{16(IP - EA)}$ and $\omega^+ \approx \frac{(IP + 3EA)^2}{16(IP - EA)}$ (Chermette 1999, Parr et al. 1999, Kirenga et al. 2022). Table 3 presents the determined chemical descriptors for the analysed dyes. Low IP and higher EA values are necessary for the injection of electrons and holes, respectively. The μ provides insights into the charge transfer pattern within the system's ground state geometry, while the η reflects the dyes' resistance to intramolecular charge transfer. Lower η is advantageous for promoting enhanced charge transfer and separation. The ω combines the electrophile's inclination to acquire additional electronic charge influenced by μ^2 and the system's resistance to exchanging electronic charge as described by η. Electrophilicity, therefore, represents the stabilization energy of the dyes. The electroaccepting and electrodonating powers assess the feasibility of withdrawing or accepting fractional electron charges, with higher values being desirable.

Table 3: Global reactivity descriptors; ionization potential (IP), electron affinity (EA), chemical potential (μ), chemical hardness (η), electrophilicity index (ω), electroaccepting power (ω^+), and electrodonating power (ω^-) of the studied dyes (in eV)

Dyes	IP	EA	$-\mu$	η	ω	ω^+	ω^-
MOL1	6.34	2.37	4.36	1.99	4.78	2.85	7.20
MOL2	6.24	1.96	4.10	2.14	3.93	2.15	6.25
MOL3	6.29	1.21	3.75	2.54	2.77	1.21	4.96
MOL4	6.32	2.27	4.30	2.03	4.55	2.66	6.96
MOL5	6.40	2.74	4.57	1.83	5.71	3.65	8.22
MOL6	6.35	2.47	4.41	1.94	5.01	3.05	7.46
MOL7	6.33	2.33	4.33	2.00	4.69	2.77	7.10
MOL8	6.34	2.30	4.32	2.02	4.62	2.71	7.03

The studied dyes exhibited IP values ranging from 6.24 to 6.40 eV, and EA values ranging from 1.21 to 2.74 eV. MOL5 exhibits the highest value of EA, indicating its superior electron accepting ability and fast electron transfer rate, while the lowest value is observed for MOL3.

Figure 4 is a visual representation that illustrates the correlation between EA and IP. It is a useful qualitative descriptor tool for assessing the electron accepting and donating abilities of molecules by utilizing both the IP and EA values (Galano et al. 2010). The diagram is divided into four quadrants: Quadrant I (strong acceptor, weak donor), Quadrant II (weak acceptor, weak donor), Quadrant III (weak acceptor, strong donor), and Quadrant IV (strong acceptor, strong donor). The findings revealed that MOL1, MOL5, MOL6, MOL7, and MOL8 were situated in the first quadrant of the FEDAM, indicating their classification as good electron acceptors and poor electron donors. This finding is in line with the results obtained for the free energies of charge injection calculations.

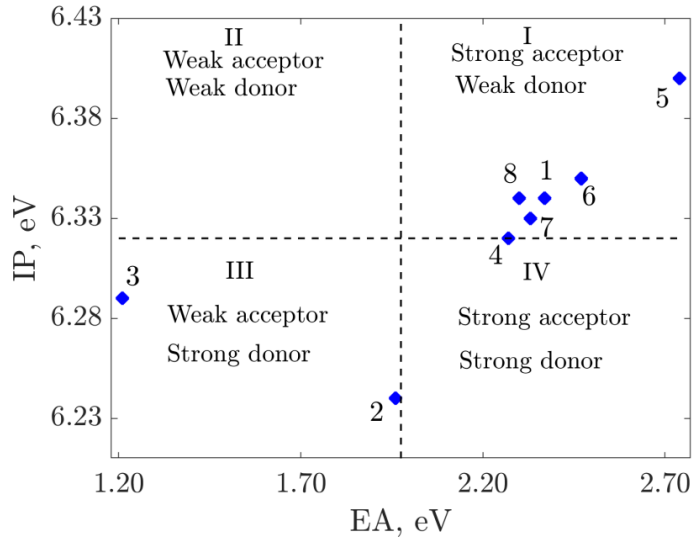

Figure 4: The full-electron-donor-acceptor map (FEDAM) for studied dyes, where the numerals 1 to 8 correspond to MOL1 to MOL8, respectively.

The molecules that demonstrated a higher driving force of charge injection (MOL2 and MOL3) were found to possess a strong donating character, this due to upshifted HOMO energies. MOL4 was identified at the boundary between Quadrant 1 and Quadrant IV, indicating that the molecule maintains a delicate equilibrium between the two states. It

is noteworthy that none of the investigated dyes fell within the region of weak donors/acceptors. Contrary to the chemical hardness, the remaining chemical descriptors in Table 3 follow an increasing order: MOL3 < MOL2 < MOL4 < MOL8 < MOL7 < MOL1 < MOL6 < MOL5. A lower chemical hardness of the sensitizers indicates a more efficient charge transfer process.

Conclusion

This study was conducted to investigate the influence of anchoring groups on the optoelectronic properties of selected sensitizers. Density functional theory and time-dependent density functional theory methods were employed to systematically analyse the dyes. The examined dyes displayed distinct absorption bands in the visible and near-infrared regions. The lower energy peaks, ranging from 498 nm to 576 nm, corresponded to the $s_0 \rightarrow s_1$ transition from the HOMO to the LUMO. The HOMO to LUMO transitions were attributed to localized $\pi \rightarrow \pi^*$ electron migration from the donor to the acceptor unit, while the higher energy bands were associated with $n \rightarrow \pi^*$ transitions. The red-shift observed in the electronic spectra correlated positively with the shift in HOMO energies, while the correlation with LUMO energies was weaker. Most of the studied dyes exhibited favourable conditions for spontaneous charge transfer, indicated by negative values of the free energy of charge injection. However, MOL5 and MOL6 deviated from this trend, suggesting less favourable charge transfer properties that require further optimization. Additionally, the results showed that all dyes were capable of spontaneous regeneration. The IP values of the dyes ranged from 6.24 to 6.40 eV, while the electron affinity values ranged from 1.21 to 2.74 eV. MOL5 exhibited the highest EA value, indicating superior electron accepting ability and fast electron transfer rate. Based on the presented results, the sensitizers demonstrate promising potential for application in DSSCs. Therefore, they are considered as strong candidates that merit further experimental synthesis and testing.

Acknowledgements

The author would like to acknowledge the valuable contributions of Melkizedeck Tsere for his role during the conceptualization of the idea and Fortunatus Jacob and Lucy Kiruri for their assistance in reviewing and editing the manuscript.

References

Arkan F, Izadyar M and Nakhaeipour A 2015 A quantum chemistry study on the performance of porphyrin-based solar cell sensitisers; zinc and anchor group position effects. *Mol. Phys.* 113(23): 3815-3825.

Barone V and Cossi M 1998 Quantum calculation of molecular energies and energy gradients in solution by a conductor solvent model. *J. Phys. Chem. A*. 102(11): 1995-2001.

Becke AD 1996 Density-functional thermochemistry. IV. A new dynamical correlation functional and implications for exact-exchange mixing. *J. Chem. Phys.* 104(3): 1040-1046.

Cammi R and Tomasi J 1995 Remarks on the use of the apparent surface charges (ASC) methods in solvation problems: Iterative versus matrix-inversion procedures and the renormalization of the apparent charges. *J. Comput. Chem*. 16(12): 1449-1458.

Chermette H 1999 Chemical reactivity indexes in density functional theory. *J. Comput. Chem*. 20(1): 129-154.

Cui Y, Wu Y, Lu X, Zhang X, Zhou G, Miapeh FB, Zhu W and Wang ZS 2011 Incorporating benzotriazole moiety to construct D–A−π–A organic sensitizers for solar cells: significant enhancement of open-circuit photovoltage with long alkyl group. *Chem. Mater*. 23(19): 4394-4401.

Deogratias G, Al-Qurashi OS and Wazzan N 2023 Optical and electronic properties enhancement via chalcogenides: promising materials for DSSC applications. *J. Mol. Model.* 29(4): 86.

Deogratias G, Al-Qurashi OS, Wazzan N, Pogrebnaya T and Pogrebnoi A 2020a Effects of heteroatoms in π-conjugated linkers on the optical and electronic

properties of modified triphenylamine based dyes: towards DSSCs' applications. *J. Mol. Model*. 26(10): 1-15.

Deogratias G, Al-Qurashi OS, Wazzan N, Pogrebnaya T and Pogrebnoi A 2022 Effect of substituent in the acceptor on optical and electronic properties of triphenylamine based dyes: A density functional theory/time-dependent density functional theory investigation. *Mater. Sci. Semiconduct. Process.* 150: 106935.

Deogratias G, Al-Qurashi OS, Wazzan N, Seriani N, Pogrebnaya T and Pogrebnoi A 2020b Investigation of optoelectronic properties of triphenylamine-based dyes featuring heterocyclic anchoring groups for DSSCs' applications: a theoretical study. *Struct. Chem.*31: 2451-2461.

Deogratias G, Seriani N, Pogrebnaya T and Pogrebnoi A 2020c Tuning optoelectronic properties of triphenylamine based dyes through variation of pi-conjugated units and anchoring groups: A DFT/TD-DFT investigation. *J. Mol. Graph. Model*. 94: 107480.

Elmorsy MR, Su R, Fadda AA, Etman H, Tawfik EH and El-Shafei A 2018 Molecular engineering and synthesis of novel metal-free organic sensitizers with D-π-A-π-A architecture for DSSC applications: the effect of the anchoring group. *Dyes Pigments* 158: 121-130.

Fujisawa JI, Eda, T and Hanaya M 2017 Comparative study of conduction-band and valence-band edges of TiO_2, $SrTiO_3$, and $BaTiO_3$ by ionization potential measurements. *Chem. Phys. Lett*. 685: 23-26.

Galano A, Vargas R and Martínez A 2010 Carotenoids can act as antioxidants by oxidizing the superoxide radical anion. *Phys. Chem. Chem. Phys.* 12(1): 193-200.

Frisch, MJ, Trucks GW, Schlegel HB, Scuseria GE Robb MA, Cheeseman JR, Scalmani G, Barone V, Petersson GA, Nakatsuji H, Li X, Caricato M, Marenich A, Bloino J, Janesko BG, Gomperts R, Mennucci B, Hratchian HP, Ortiz JV, Izmaylov AF, Sonnenberg JL, Williams-Young D, Ding F, Lipparini F, Egidi F, Goings J, Peng B, Petrone A, Henderson T, Ranasinghe D, Zakrzewski VG, Gao J, Rega N, Zheng G, Liang W, Hada M, Ehara M, Toyota K, Fukuda R, Hasegawa J, Ishida M, Nakajima T, Honda Y, Kitao O, Nakai H, Vreven T, Throssell K, Montgomery JA, Peralta Jr JE, Ogliaro F, Bearpark M, Heyd JJ, Brothers E, Kudin KN, Staroverov VN, Keith T, Kobayashi R, Normand J, Raghavachari K, Rendell A, Burant JC, Iyengar SS, Tomasi J, Cossi M, Millam JM, Klene M, Adamo C, Cammi R, Ochterski JW, Martin RL, Morokuma K, Farkas O, Foresman JB and Fox DJ 2016 *Gaussian 16* Gaussian, Inc. Wallingford, CT. 32: 5648-5652.

Gayathri R 2018 An experimental and theoretical investigation of the electronic structure and photoelectrical properties of 1, 4-diacetoxy-2-methylnaphthalene for DSSC application. *J. Mol. Struct.* 1166: 63-78.

Guo FL, Li ZQ, Liu XP, Zhou L, Kong FT, Chen WC and Dai SY 2016 Metal-free sensitizers containing hydantoin acceptor as high performance anchoring group for dye-sensitized solar cells. *Adv. Funct. Mater.* 26(31): 5733-5740.

Hanwell MD, Curtis DE, Lonie DC, Vandermeersch T, Zurek E and Hutchison GR 2012 Avogadro: an advanced semantic chemical editor, visualization, and analysis platform. *J. Cheminform.*4(1): 1-17.

Horiuchi T, Miura H, Sumioka K and Uchida S 2004 High efficiency of dye-sensitized solar cells based on metal-free indoline dyes. *J. Am. Chem. Soc*. 126(39): 12218-12219.

IEA 2020 *Global Energy Review* 2020 *Ukraine.[Online] https://www. iea. org/countries/ukraine [Accessed: 2020-09-10]*.

Ikpesu JE, Iyuke SE, Daramola M and Okewale AO 2020 Synthesis of improved dye-sensitized solar cell for renewable energy power generation. *Solar Energy* 206: 918-934.

Irfan A 2019 Comparison of mono- and di-substituted triphenylamine and carbazole based sensitizers $@(TiO_2)_{38}$ cluster for

dye-sensitized solar cells applications. *Comput. Theor. Chem.*1159: 1-6.

Jia HL, Peng ZJ, Gong BQ, Huang CY and Guan MY 2019 New 2D–π–2A organic dyes with bipyridine anchoring groups for DSSCs. *New J. Chem.* 43(15): 5820-5825.

Kirenga P, Mkoma SL, Mlowe S, Msambwa Y, Kiruri LW, Jacob FR, Mgaya JE, Kinunda GA, Deogratias G 2022 Influence of Heteroatoms on the Optoelectronic Properties of Triphenylamine-based Dyes for DSSCs Application: A Computational Approach. *Comput. Theor.l Chem.* 1210: 113644.

Liu S, Jiao Y, Ding Y, Fan X, Song J, Mi B and Gao Z 2020 Position engineering of cyanoacrylic-acid anchoring group in a dye for DSSC applications. *Dyes and Pigments* 180: 108470.

Lokhande PKM, Sonigara KK, Jadhav MM, Patil DS, Soni SS and Sekar N 2019 Multi-dentate carbazole based Schiff base dyes with chlorovinylene group in spacer for dye-sensitized solar cells: A combined theoretical and experimental study. *Chem. Select* 4(14): 4044-4056.

Luo GG, Lu H, Wang YH, Dong J, Zhao Y and Wu RB 2016 A D-π-A-π-A metal-free organic dye with improved efficiency for the application of solar energy conversion. *Dyes Pigments* 134: 498-505.

Maddah HA, Berry V and Behura SK 2020 Biomolecular photosensitizers for dye-sensitized solar cells: Recent developments and critical insights. *Renew. Sustain. Energy Rev.*121: 109678.

Mariotti N, Bonomo M, Fagiolari L, Barbero N, Gerbaldi C, Bella F and Barolo C 2020 Recent advances in eco-friendly and cost-effective materials towards sustainable dye-sensitized solar cells. *Green Chem.* 22(21): 7168-7218.

Miertuš S, Scrocco E and Tomasi J 1981 Electrostatic interaction of a solute with a continuum. A direct utilizaion of AB initio molecular potentials for the prevision of solvent effects. *Chem. Phys.* 55(1): 117-129.

Panneerselvam M, Kathiravan A, Solomon RV and Jaccob M 2017 The role of π-linkers in tuning the optoelectronic properties of triphenylamine derivatives for solar cell applications–A DFT/TDDFT study. *Phys. Chem. Chem. Phys*. 19(8): 6153-6163.

Parida B, Iniyan S and Goic R 2011 A review of solar photovoltaic technologies. *Renew. Sustain. Energy Rev*. 15(3): 1625-1636.

Parr RG, Szentpály LV and Liu S 1999 Electrophilicity index. *J. Am. Chem. Soc*. 121(9): 1922-1924.

Pathak A, Tomer T, Thomas KJ, Fan MS and Ho KC 2019 Fine tuning the absorption and photovoltaic properties of benzothiadiazole dyes by donor-acceptor interaction alternation via methyl position. *Electrochim. Acta* 304: 1-10.

Sharma K, Sharma V and Sharma SS 2018 Dye-sensitized solar cells: fundamentals and current status. *Nanoscale Res. Lett.* 13: 1-46.

Shkoor M, Mehanna H, Shabana A, Farhat T and Bani-Yaseen AD 2020 Experimental and DFT/TD-DFT computational investigations of the solvent effect on the spectral properties of nitro substituted pyridino [3, 4-c] coumarins. *J. Mol. Liquids* 313: 113509.

Slimi A, Hachi M, Fitri A, Benjelloun AT, Elkhattabi S, Benzakour M, Mcharfi, M, Khenfouch M, Zorkani I and Bouachrine M 2020 Effects of electron acceptor groups on triphenylamine-based dyes for dye-sensitized solar cells: Theoretical investigation. *J. Photochem. Photobiol. A: Chem.* 398: 112572.

Sun ZZ, Li QS, Sun PP and Li ZS 2015 Probing the regeneration process of triphenylamine-based organic dyes in dye-sensitized solar cells. *J. Power Sources* 276: 230-237.

Tian G, Cai S, Li X, Ågren H, Wang Q, Huang J and Su J 2015 A new D–A–π–A type organic sensitizer based on substituted dihydroindolo [2, 3-b] carbazole and DPP unit with a bulky branched alkyl chain for highly efficient DSCs. *J. Mater. Chem. A* 3(7): 3777-3784.

Wan Z, Jia C, Wang Y and Yao X 2017 A strategy to boost the efficiency of rhodanine electron acceptor for organic

dye: from nonconjugation to conjugation. *ACS Appl. Mater. Interfaces* 9(30): 25225-25231.

Wan Z, Yang J, Xia J, Shu H, Yao X, Luo J and Jia C 2021 Simple molecular structure but high efficiency: Achieving over 9% efficiency in dye-sensitized solar cells using simple triphenylamine sensitizer. *J. Power Sour.* 506: 230214.

Wang Z, Zang XF, Shen H, Shen C, Ye X, Li Q, Quan YY, Ye F, Huang ZS 2020 Dithienopyrrolobenzothiadiazole-based metal-free organic dyes with double anchors and thiophene spacers for efficient dye-sensitized solar cells. *Solar Energy*. 208: 1103-1113.

Wu F, Liu J, Li X, Song Q, Wang M, Zhong C and Zhu L 2015 D–A–A-type organic dyes for NiO-based dye-sensitized solar cells. *Eur. J. Org. Chem*. 2015(31): 6850-6857.

Xu B, Sheibani E, Liu P, Zhang J, Tian H, Vlachopoulos N, Boschloo G, Kloo L, Hagfeldt A, Sun L 2014 Carbazole-based hole-transport materials for efficient solid-state dye-sensitized solar cells and perovskite solar cells. *Adv. Mater*. 26(38): 6629-6634.

Yanai T, Tew DP and Handy NC 2004 A new hybrid exchange–correlation functional using the Coulomb-attenuating method (CAM-B3LYP). *Chem. Phys. Lett*. 393: 51-57.

Zhang H, Chen ZE and Tian HR 2020 Molecular engineering of metal-free organic sensitizers with polycyclic benzenoid hydrocarbon donor for DSSC applications: The effect of the conjugate mode. *Solar Energy* 198: 239-246.

Zhang H, Iqbal Z, Chen ZE and Hong Y 2018a Effects of various heteroatom donor species on the photophysical, electrochemical and photovoltaic performance of dye-sensitized solar cells. *Electrochim. Acta* 290: 303-311.

Zhang J, Zhu HC, Zhong RL, Wang L and Su ZM 2018b Promising heterocyclic anchoring groups with superior adsorption stability and improved IPCE for high-efficiency noncarboxyl dye sensitized solar cells: A theoretical study. *Org. Electron.* 54: 104-113.

Zhao L, Wang G, Liu Y and Yang Z 2021 First principles design novel D5 derivative dyes with excellent acceptors for highly efficient dye-sensitized solar cells. *Comput. Theor. Chem.* 1203: 113374.